Enhancing Sensor Pattern Noise for Source Camera Identification: An Empirical Evaluation

Bei-bei Liu *
School of Computing Science
Newcastle University,UK
beibei.liu2@ncl.ac.uk

Xingjie Wei
School of Computing Science
Newcastle University,UK
xingjie.wei@ncl.ac.uk

Jeff Yan
School of Computing Science
Newcastle University,UK
jeff.yan@ncl.ac.uk

ABSTRACT

The sensor pattern noise (SPN) based source camera identification technique has been well established. The common practice is to subtract a denoised image from the original one to get an estimate of the SPN. Various techniques to improve SPN's reliability have previously been proposed. Identifying the most effective technique is important, for both researchers and forensic investigators in law enforcement agencies. Unfortunately, the results from previous studies have proven to be irreproducible and incomparable —there is no consensus on which technique works the best. Here, we extensively evaluate various ways of enhancing the SPN by using the public "Dresden" database. We identify which enhancing methods are more effective and offer some insights into the behavior of SPN. For example, we find that the most effective enhancing methods share a common strategy of spectrum flattening. We also show that methods that only aim at reducing the contamination from image content do not lead to satisfying results, since the non-unique artifacts (NUA) among different cameras are the major troublemaker to the identification performance. While there is a trend of employing sophisticate methods to predict the impact of image content, our results suggest that more effort should be invested to tame the NUAs.

Categories and Subject Descriptors

I.4 [**Image processing and computer vision**]: Miscellaneous

General Terms

Algorithms, Experimentation, Performance, Security

Keywords

Digital Image Forensics; Sensor Pattern Noise; Source Camera Identification

*Liu is also affiliated with the School of Electronic and Information Engineering, South China University of Technology.

IH&MMSec'15, June 17–19, 2015, Portland, Oregon, USA.

ACM 978-1-4503-3587-4/15/06 ...$15.00.
DOI: http://dx.doi.org/10.1145/2756601.2756614.

1. INTRODUCTION

It is well known that the sensor pattern noise (SPN) intrinsically embedded in a digital image can be employed to identify the source camera with which the image was taken. The SPN based source camera identification is among the most promising digital forensic techniques. By extracting the SPN from a suspect image, the source camera can be tracked down, providing a critical clue or evidence for law enforcement agencies.

In their seminal work [9], Lukáš et al. have laid down the fundamental scheme for SPN based source camera identification, which consists of three parts: extracting the SPN from an image, composing the reference pattern noise (RPN) for a camera and establishing the relation between an image and a camera. Abundant studies are devoted to improving the performance of SPN based source identification. Some of them focus on finding the optimal denoising filter for SPN extraction [1, 4, 15, 5], while some others focus on increasing the reliability of the extracted SPN (SPN enhancing).

It is generally recognised that the deterioration in SPN is caused by two sources, one is the non-unique artifacts (NUA) shared among different cameras and the other is the interference from image content. There are various SPN enhancing methods proposed in the literature. Some of these methods aim at eliminating the NUA while others try to counteract contamination introduced by image content. Evaluating differences in performance between these methods is important, but currently unfeasible due to inconsistent evaluation conditions across various studies —in other words, it is not yet clear which method works the best. For example, most studies are based on self-built datasets, making it impossible to reproduce and intercompare the reported results. Apparently different selections of cameras and images have an impact on the results.

In this work, we conduct an extensive evaluation on a range of SPN enhancing methods using a third-party public database. To the best of our knowledge, our work is novel in several aspects. (1) It is the first and most comprehensive evaluation of SPN enhancing. We evaluate 13 different enhancing schemes,consisting of the most typical methods and their combinations. (2) The results are obtained on a third-party database with consistent evaluation procedures and conditions. The previously reported experimental results are hardly intercomparable, because most experiments are conducted on self-built datasets using different measurements. (3) The scale of our experiment is significantly larger than those of related works in terms of the number of cameras and images involved. Particularly, the wide range of camera brands and models provides valuable samples for investigating the inter-camera similarities. (4) Our evaluation strategy differentiates between the enhancement techniques applied to the RPN of the camera and that applied to the SPN of the test image. This strategy has the advantage of identifying which part of the enhancement is actually working. The mix of the two types of enhancements is a cause of ambiguity in extant literature.

The rest of this paper is organised as follows. Section 2 briefly examines the fundamental scheme of SPN based source identification and related enhancing methods. Section 3 describes the setup of our evaluation. The results are presented and analysed in Section 4. Section 5 concludes the paper.

2. BACKGROUND AND RELATED WORKS

In this section, we first review the fundamental scheme of SPN based source identification introduced in [9]. Then we briefly describe some typical enhancing methods that can be categorised into two groups: methods to enhance the RPN of a camera and methods to enhance the SPN extracted from a test image.

2.1 The fundamental scheme

In [9], Lukáš et al. established the function of SPN as an identification of its source camera. For an image $\mathbf{I}$, the SPN $\mathbf{n}$ of which can be approximated by the noise residual extracted from the original image:

$$\mathbf{n} = \mathbf{I} - F(\mathbf{I}) \tag{1}$$

where a wavelet based filter [14] is recommended as the denoising filter F. For a camera C, a reference pattern noise (RPN) $\mathbf{r}$ of which can be achieved by averaging the SPNs of multiple images captured by C.:

$$\mathbf{r} = \sum_{i=1}^{L} \mathbf{n}_i / L \tag{2}$$

where L is the number of images involved in composing the RPN and recommended to be no less than 50. It is also suggested that flat field images or blue sky images are preferred for producing the RPN. To decide whether an image is taken by a particular camera, normalised cross-correlation (NCC) between the SPN and the RPN is calculated:

$$\rho = corr(\mathbf{n}, \mathbf{r}) = \frac{(\mathbf{n} - \bar{\mathbf{n}}) \cdot (\mathbf{r} - \bar{\mathbf{r}})}{\|\mathbf{n} - \bar{\mathbf{n}}\| \|\mathbf{r} - \bar{\mathbf{r}}\|} \tag{3}$$

The image is considered as being captured by the camera if the correlation ρ exceeds a predefined threshold.

Note that in a later work from the same research team [3], Eq.(2) is replaced by a maximum-likelihood estimator to estimate the PRNU(photo-response non-uniformity) of a camera. The NCC measurement of Eq.(4) is also suggested to be replaced by the peak to correlation energy (PCE) ratio in [8]. However, since we exploit flat field images (image of approximately constant intensity) in our experiments to compose the RPN, there is no much difference between using the PRNU estimator of [3] and the simple averaging method of Eq.(2). Besides, probably due to its simplicity, the NCC measurement is still widely adopted in the literature, especially in the related studies that we are evaluating. Therefore, in this work, we stick to using Eq.(1)∼(3) as the baseline scheme. We leave it to the future work to find out how the results are affected when using different detectors such as PCE.

2.2 Enhancing the RPN of a camera

The motivation of enhancing the RPN of a camera is to remove the linear pattern and non-unique artifacts shared among different cameras. Although the inter-camera similarities has been recognized earlier in [9], it is in [3] where two specific operations —zero-mean and Wiener filtering are first proposed to tackle these undesired artifacts.

Zero-mean (ZM) operation [3]: It is believed that linear pattern will be introduced into the RPN due to the color interpolation in cameras as well as the row-wise and column-wise operation of sensors and processing circuits. To remove such linear pattern, the RPN obtained with Eq.(2) is processed by zeroing out the means of its columns and rows.

Wiener filtering (WF) operation [3]: It is also observed that the blockiness artifacts caused by JPEG compression may affect the estimated RPN. As such, a Wiener filter in the Fourier domain is applied to the RPN $\mathbf{r}$ to suppress the peaks and ridges in its spectrum:

$$WF(\mathbf{r}) = \mathcal{F}^{-1}\{\mathcal{F}(\mathbf{r}) - W(\mathcal{F}(\mathbf{r}))\} \tag{4}$$

where $\mathcal{F}$ indicates the Fourier transform and W is a 3×3 Wiener filter.

The above two operations were introduced at a very early stage of the research of SPN. After an extensive review of related works, we observed that while the ZM operation has been adopted by many, the WF operation has been frequently neglected. However, as will be seen in Section 4,we show that the contribution of the WF operation has been largely undervalued.

Phase RPN [11]: Kang et al. propose to use a 'phase RPN'in order to eliminate the various artifacts [11]. Specifically, the SPNs of the reference images are first transformed to the Fourier domain, the whitened spectra are averaged before being transformed back to the spatial domain:

$$\mathbf{r}_{\text{phase}} = real(\mathcal{F}^{-1}(\frac{\sum_{i=1}^{L} \mathbf{w}_i}{L})) \tag{5}$$

where $\mathcal{F}$ denotes the Fourier transform, and $\mathbf{w} = \mathcal{F}(\mathbf{n}) / \|\mathcal{F}(\mathbf{n})\|$ is the phase component of the SPN $\mathbf{n}$. The phase RPN and the WF operation share the spirit of spectrum flattening. Our study shows that the two operations indeed give very close performances.

2.3 Enhancing the SPN of a test image

Li first points out in [12] that the SPN of an image can be contaminated by the image content. Image details such as edges and textures are visible in the SPN. Believing that these content artifacts are harmful to the SPN, a number of methods have been proposed to counteract such scene interference.

Attenuation models [12]: Based on the assumption that for each component in the SPN $\mathbf{n}$, the larger magnitude it has, the more likely it is contaminated by scene details. As such, in [12], Li proposes five attenuation models to assign less significance weighting factors to the large components. In particular, Li reports the best result is achieved on the following model (the Model 5 in the source study):

$$\mathbf{n}_{\mathrm{att}(i,j)} = \begin{cases} e^{-0.5\mathbf{n}^2(i,j)/\alpha^2}, & \text{if } \mathbf{n}(i,j) \geq 0 \\ -e^{-0.5\mathbf{n}^2(i,j)/\alpha^2}, & \text{otherwise} \end{cases} \tag{6}$$

where α is the model parameter. In our evaluation we follow the optimal value suggested by the original paper. We noticed that there is an ambiguity about in which domain the attenuation model should be applied. The original proposition of [12] is to conduct the attenuation in the wavelet domain. However, there also sees implementation in other studies that applies the attenuation model in the spatial domain. For completeness, we include both implementations in our experiments.

Confidence weighting [13]: While the attenuation model in [12] decides the weight of a component simply by its magnitude, there are a few works that propose to use the content adaptive weighting scheme. This scheme weights against those image regions that we have less confidence in its SPN, typically being edge and highly textured regions. For example, image gradient magnitudes are exploited in [13] while a pair of intensity and texture features are used in [2]. Since some critical information for implementation is implicit in [2], we are not including it in our evaluation but use [13] to represent this line of work. The weight w for each pixel p is calculated in [13] as:

$$w(p) = G(\sigma) * \frac{1}{(1 + \|\nabla I(p)\|)} \tag{7}$$

where $G(\sigma)$ is a Gaussian kernel and ∇ denotes the gradient operator.

Whitening operation [10]: Similar to the idea of phase RPN, Kang et al. also propose to whiten the SPN of a test image[10]. A whitened SPN $\mathbf{n}_{\mathrm{wh}}$ is obtained by:

$$\mathbf{n}_{\mathrm{wh}} = \mathcal{F}^{-1}\left(\frac{\mathcal{F}(\mathbf{n})}{\|\mathcal{F}(\mathbf{n})\|}\right) \tag{8}$$

3. EXPERIMENTAL SETUP

3.1 Database

Our experiments use the “Dresden” image database [6] which features over 14,000 images acquired under controlled conditions with a wide range of cameras (73 cameras of 25 different models).In addition to indoor and outdoor natural images, the database provides a number of flat field images for each camera, which can be used to compose the camera’s RPN. The number of flat field images per camera varies, and this may influence the quality of the RPN obtained. For the sake of equality, we only use those cameras with 50 flat field images available. As such, 46 cameras are included in our experiments, spanning 15 models and with 9268 test images available in total.The details of the cameras are listed in Table 2 in the Appendix.

Three features, among others, make the “Dresden” database suitable for the purpose of our research. First, as a third-party public database, “Dresden” exhibits no preference for any particular algorithms, which enables an objective assessment. Second, for most models multiple devices are available, which serves as excellent specimens for studying the NUA shared among different cameras. Last, some images captured by different cameras have highly similar scene content, i.e. the images were taken at several fixed scenarios with varying cameras. Such a setting is rare in the literature but crucial to tease apart different factors that affect the SPN.

3.2 Evaluation methodology

We use the flat field images in the database to compose the RPN of each camera. The indoor and outdoor images captured with each camera are used as test images. Following the most widely adopted practise in literature, we first convert each image, either flat field or natural, to grayscale and then cut from center for a 512×512 block. We acknowledge that the image size as well as the JPEG compression level may have an impact on the performance. We leave it to future work to include more varying factors in the evaluation.

We assess how well the test images are matched with their true source cameras when different enhancing methods are applied. The camera identification problem is generally formulated as a signal detection hypothesis and, in forensic scenarios, a low False Positive Rate (FPR) is particularly important. Thus, we employ the experimental TPR for a fixed FPR of 10^{-3} as the evaluation measurement. More specifically, for each camera, we first determine a threshold for the NCC of Eq.(3) so that no more than 0.1% of the non-matching images are falsely judged as matching images. We then caculate the True Positive Rate (TPR) under this threshold, i.e. how many matching images are correctly identified. Finally, an overall TPR is obtained by averaging over the 46 cameras.

We divide our tests into four groups consisting of different combinations of methods which have been examined in Section 2, as listed in Table 1. Group 1 is the baseline scheme where the SPN and the RPN obtained with Eq.(1) and Eq.(5) do not undergo any enhancing operation. In Group 2, the RPNs remain un-processed while the SPNs of test images are enhanced with different methods. In Group 3, the SPNs of test images remain un-processed while the RPNs undergo different operations. In Group 4, enhancing operations are applied to both the RPNs of cameras and the SPNs of test images.

4. RESULTS AND ANALYSIS

The overall TPR and the corresponding rank obtained with each enhancing scheme are given in the last two columns of Table 4. The results not only reveal the most effective enhancing scheme but also clarify some misconceptions in the literature.

4.1 Which is the most effective?

The results show that among the 13 schemes evaluated, the top scheme is G4-3 which combines the confidence weighting method proposed by McCloskey [13] and the ZM and WF operations proposed by Chen et al. [3], achieving a TPR of 84.79%. It is also clear from Table 4 that some other schemes (G2-4,G3-2,G3-3,G3-4,G4-1,G4-2,G4-4) also perform well, achieving TPRs between 82.27% and 84.79%. All the well-performing schemes share a common strategy: they all employ spectrum flattening. This suggests that the whitening methods proposed by Kang et al.[10, 11] and the Wiener filtering operation proposed by Chen et al.[3] are both effective. Interestingly, while spectrum flattening is effective, it does not make much difference when applied to both the RPN and the SPN at the same time (G4-4).

Table 1: The 13 schemes being evaluated and the TPRs obtained at a fixed FPR of 10^{-3}.

	Scheme ID	RPN of camera	SPN of test image	TPR for FPR=10^{-3}	Rank
Group 1	G1-1	Basic	Basic	63.65 %	11
Group 2	G2-1	Basic	Attenuation in wavelet domain	56.16 %	13
	G2-2	Basic	Attenuation in spatial domain	59.69 %	12
	G2-3	Basic	Confidence weighting	65.47 %	10
	G2-4	Basic	Whitening	83.94 %	2
Group 3	G3-1	Zero-mean (ZM)	Basic	71.06 %	9
	G3-2	Wiener filtering (WF)	Basic	83.43 %	4
	G3-3	ZM+WF	Basic	83.69 %	3
	G3-4	Phase RPN	Basic	82.27 %	8
Group 4	G4-1	ZM+WF	Attenuation in wavelet domain	83.09 %	7
	G4-2	ZM+WF	Attenuation in spatial domain	83.30 %	5
	G4-3	ZM+WF	Confidence weighting	84.79 %	1
	G4-4	ZM+WF	Whitening	83.13 %	6

Note that although G4-3 achieves the highest TPR among all, the confidence weighting operation of [13] does not work well alone (G2-3). This confirms our discovery that spectrum flattening is key to an effective enhancement. This demonstrates an advantage of our evaluation strategy, which differentiates between enhancements applied to the RPN and those applied to the SPN. This way, we are able to pinpoint the element that actually works.

Regarding to the zero-mean and the Wiener filtering operations, both proposed by Chen et al.[3], a close-up of Group 3 shows that Wiener filtering plays a more important role than the zero-mean operation in removing artifacts from the camera RPN. The TPR obtained by applying Wiener filtering alone (G3-2) is notably higher than the TPR obtained by applying zero-mean alone (G3-1). Moreover, applying both of them (G3-3) does not significantly increase the TPR on top of G3-2.

4.2 Is the baseline method the worst?

Table 1 shows that the baseline method (G1-1) achieves a lower TPR than most of the other methods, which confirms the necessity of enhancement. However, the attenuation models proposed by Li [12], applied either in the wavelet (G2-1) or the spatial domains (G2-2), produce slightly lower TPRs than the baseline method. A similar weak performance of the attenuation model is also observed in other studies [10, 11]. To explain this, we examine difference introduced by individual cameras. We find that the low TPR is mainly caused by the 8 Sony cameras (C39-C46, Table 2) for which inter-camera correlations exhibit a visible increase after application of attenuation. We conjecture that this is because Eq.(6) magnifies the small magnitude components. As a result, rather than being removed or compressed, the originally weak non-unique artifacts in the SPN have been reinforced, which leads to a worse source identification result.

4.3 The impact of non-unique artifacts

In this section we demonstrate why some enhancing methods work well while others do not. The ideal SPN for source identification should exhibit high correlation with the RPN of the true source camera but low correlation with the RPN of other cameras. We examine how the two types of correlation values are affected by different enhancing methods.

For the ith camera C_i, we average the correlation values computed between its RPN and the SPNs of test images from the jth camera C_j:

$$\bar{\rho}_{i,j} = \frac{\sum_{k=1}^{N_j} corr(\mathbf{r}_i, \mathbf{n}_j^k)}{N_j} \tag{9}$$

where $\mathbf{r}_i$ is the RPN of camera C_i, $\mathbf{n}_j^k$ is the SPN of the kth test image of camera C_j and N_j is the total number of test images available for camera C_j.

The pairwise average values obtained with Eq.(9) are displayed as intensity images. The off-diagonal components, which indicate correlations between non-matching cameras and images, are supposed to be as dark as possible (close to zero). However, as can be seen from Fig.1, there exist apparent bright off-diagonal components when neither the RPN or SPN is enhanced. These stains illustrate the well-known non-unique artifacts shared among different cameras.

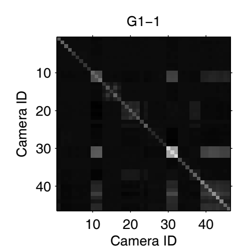

Figure 1: Intensity image displaying the average correlation values (Eq.9) for G1-1.

Fig.2 demonstrates what happens after enhancement. As can be seen, the off-diagonal stains hardly shift in (a),(b) and (c) which correspond to the two attenuation models and the confidence weighting method. Recall that these three methods all perform poorly in our evaluation (see Table 1). The reason of their poor performance turns out to be the failure to remove the NUAs. It is reasonable to deduce that the removal of NUA is most crutial to a reliable source identification. On the other hand, most of the off-diagonal stains vanish in (d) and (f)∼(l) where at least one type of spectrum flattening operation is applied, indicating that the success of spectrum flattening is mainly attributed to the removal of NUAs across cameras. Note that the stains in (e) do not

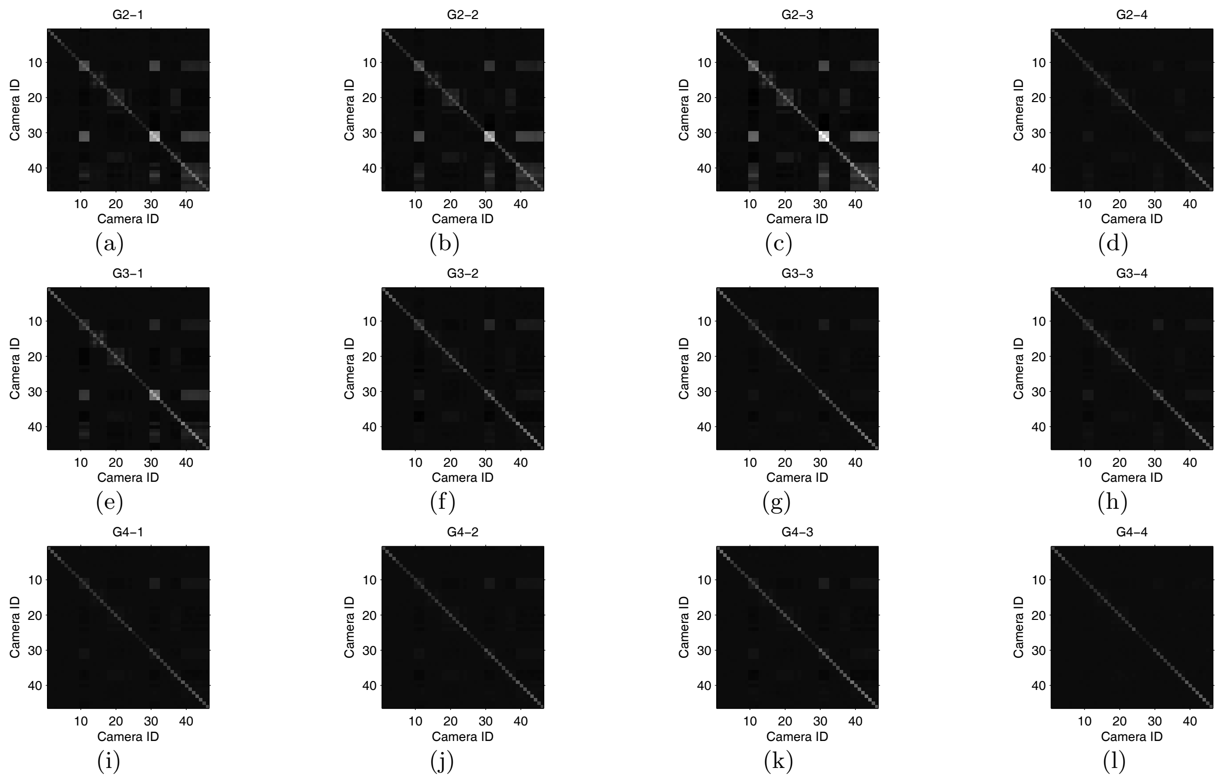

Figure 2: Intensity images displaying the average correlation values (Eq.9) for Group 2, 3 and 4.

vanish as much as those in (d) and (f)∼(l), which tallies with our finding that the zero-mean operation is less effective than spectrum flattening.

4.4 Variability across different cameras

Our final observation is that the performances of individual cameras (not displayed due to space limitation) vary considerably. The individual TPR fluctuates dramatically from camera to camera. For some cameras (e.g. the Casio cameras in Table 2), the TPR is as low as about 33%, while for some others (e.g. the Canon cameras in Table 2), it can easily reach 100% without any form of enhancing. It is important to note that the observed variability cannot be attributed to other factors than the intrinsic characteristics of the individual cameras: the 'Dresden'database is specially designed so that each camera in the database captures almost the same scenes. On the one hand, the recognition of camera variations highlights the importance of reporting results on third-party public database for future studies. On the other hand, it also shows that we are far from comprehensively understanding the behavior of the SPN of various cameras. It deserves a further investigation into the reason for the observed variability across different cameras in the future.

5. SUMMARY

There are various methods to improve the reliability of the SPN based source camera identification technique, both for the SPN of an image and the RPN of a camera. However, the more methods on the shelves, the more difficult it is to pinpoint the best one. Unfortunately, the results reported in the literature are largely irreproducible and impossible to compare with each other because many factors vary from one study to another. This work is the first attempt to provide an independent assessment of the effectiveness of various SPN enhancing methods. We have evaluated a total of 13 schemes consisting of various combinations of representative enhancing methods. We explicitly differentiate between the enhancement applied to the camera RPN and that to the SPN of test image, hereby clarifying which of these enhancements actually work. Apart from revealing the most effective enhancing methods, our evaluation also clear up some misconceptions and identifies promising directions for future studies. We summarise our findings as follows:

(1) The combination of the confidence weighting method [13] and the zero-mean and Wiener filtering operations [3] achieves the best performance. Importantly, this result is primarily attributed to the effect of Wiener filtering, since neither the zero-mean operation nor weighting performs well alone.

(2) Our evaluation results demonstrate a clear division between the schemes that involve spectrum flattening and those that do not, suggesting that spectrum flattening is a very effective enhancing method. We also clarify that the Wiener filtering is more critical than the zero-mean operation, although the former has frequently been neglected in related studies. Besides, it does not seem to matter whether the spectrum flattening operation is applied to the RPN of camera, to the SPN of test image, or both. This suggests that we do not have to flatten the spectra of the two at the same time to guarantee a reliable results. This result is particularly relevant to large-scale forensic investigations, since spectrum manipulation is computationally expensive.

(3) Our evaluation shows that the major troublemaker to SPN based source identification is the non-unique artifacts, rather than the contamination introduced by image content. Low ranking schemes in our evaluation commonly failed to remove the NUAs across cameras. The image content influences the SPN mainly in the sense of squeezing out the useful SPN components, which is more likely to cause a true match to be falsely rejected than a wrong match to be falsely accepted. The NUAs, on the other hand, are mainly responsible for the false acceptance. Since a low false acceptance rate is critical in forensic investigations, it is more important to counter the influence of NUAs.

(4) Different cameras show varying responses to different enhancements. There is also a number of cameras on which none of the state-of-the-art enhancing methods can achieve satisfying results, which corroborates the observation in [7]. This variability reflects the complexity of camera making and highlights the further need for identifying novel artifacts and corresponding countermeasures.

6. ACKNOWLEDGMENTS

We thank Ahmet Emir Dirik for helpful comments. This research was supported by the EU programme on Prevention of and Fight against Crime (ISEC) —the Novel Image/photo Forensic Tools for fighting against child pornography (NIFTy) project (HOME/2012/ISEC/AG/INT/4000003892).

7. REFERENCES

[1] I. Amerini, R. Caldelli, V. Cappellini, F. Picchioni, and A. Piva. Analysis of denoising filters for photo response non uniformity noise extraction in source camera identification. In *Digital Signal Processing, 2009 16th International Conference on*, pages 1–7. IEEE, 2009.

[2] L.-H. Chan, N.-F. Law, and W.-C. Siu. A confidence map and pixel-based weighted correlation for prnu-based camera identification. *Digital Investigation*, 10(3):215–225, 2013.

[3] M. Chen, J.Fridrich, M.Goljan, and J.Lukas. Determining image origin and integrity using sensor noise. *IEEE Trans.Inf.Forensics Security*, 3(1):74 – 90, 2008.

[4] G. Chierchia, S. Parrilli, G. Poggi, C. Sansone, and L. Verdoliva. On the influence of denoising in prnu based forgery detection. In *Proceedings of the 2nd ACM workshop on Multimedia in forensics, security and intelligence*, pages 117–122. ACM, 2010.

[5] A. Cortiana, V. Conotter, G. Boato, and F. G. De Natale. Performance comparison of denoising filters for source camera identification. In *IS&T/SPIE Electronic Imaging*, pages 788007–788007. International Society for Optics and Photonics, 2011.

[6] T. Gloe and R. Böhme. The dresden image database for benchmarking digital image forensics. *Journal of Digital Forensic Practice*, 3(2-4):150–159, 2010.

[7] T. Gloe, S. Pfennig, and M. Kirchner. Unexpected artefacts in prnu-based camera identification: a'dresden image database'case-study. In *Proceedings of the on Multimedia and security*, pages 109–114. ACM, 2012.

[8] M. Goljan and J. Fridrich. Camera identification from cropped and scaled images. In *Electronic Imaging 2008*, pages 68190E–68190E. International Society for Optics and Photonics, 2008.

[9] J.Lukas, J.Fridrich, and M.Goljan. Digital camera identification from sensor pattern noise. *IEEE Trans.Inf.Forensics Security*, 1(2):205 – 214, 2006.

[10] X. Kang, Y. Li, Z. Qu, and J. Huang. Enhancing roc performance of trustworthy camera source identification. In *IS&T/SPIE Electronic Imaging*, pages 788009–788009, 2011.

[11] X. Kang, Y. Li, Z. Qu, and J. Huang. Enhancing source camera identification performance with a camera reference phase sensor pattern noise. *IEEE Trans.Inf.Forensics Security*, 7(2):393 – 402, 2012.

[12] C.-T. Li. Source camera identification using enhanced sensor pattern noise. *IEEE Trans.Inf.Forensics Security*, 5(2):280 – 287, 2010.

[13] S. McCloskey. Confidence weighting for sensor fingerprinting. In *Computer Vision and Pattern Recognition Workshops, 2008. CVPRW'08. IEEE Computer Society Conference on*, pages 1–6, 2008.

[14] M. Mihcak, I. Kozintsev, and K. Ramchandran. Spatially adaptive statistical modeling of wavelet image coefficients and its application to denoising. In *Acoustics, Speech, and Signal Processing, 1999. Proceedings., 1999 IEEE International Conference on*, volume 6, pages 3253–3256, 1999.

[15] W. van Houten and Z. Geradts. Using anisotropic diffusion for efficient extraction of sensor noise in camera identification. *Journal of forensic sciences*, 57(2):521–527, 2012.

APPENDIX

Table 2: 46 cameras used in our evaluation

ID	Name	ID	Name
C1	Canon_Ixus55	C24	Pentax_W60
C2	Canon_Ixus70_0	C25	Praktica_DCZ5p9_0
C3	Canon_Ixus70_1	C26	Praktica_DCZ5p9_1
C4	Canon_Ixus70_2	C27	Praktica_DCZ5p9_2
C5	Casio_EXZ150_0	C28	Praktica_DCZ5p9_3
C6	Casio_EXZ150_1	C29	Praktica_DCZ5p9_4
C7	Casio_EXZ150_2	C30	Rollei_7325XS_0
C8	Casio_EXZ150_3	C31	Rollei_7325XS_1
C9	Casio_EXZ150_4	C32	Rollei_7325XS_2
C10	Fujifilm_J50_0	C33	Samsung_L74_0
C11	Fujifilm_J50_1	C34	Samsung_L74_1
C12	Fujifilm_J50_2	C35	Samsung_L74_2
C13	Nikon_S710_0	C36	Samsung_NV15_0
C14	Nikon_S710_1	C37	Samsung_NV15_1
C15	Nikon_S710_2	C38	Samsung_NV15_2
C16	Nikon_S710_3	C39	Sony_H50_0
C17	Nikon_S710_4	C40	Sony_H50_1
C18	Olympus_u1050_0	C41	Sony_T77_0
C19	Olympus_u1050_1	C42	Sony_T77_1
C20	Olympus_u1050_2	C43	Sony_T77_2
C21	Olympus_u1050_3	C44	Sony_T77_3
C22	Olympus_u1050_4	C45	Sony_W170_0
C23	Pentax_A40_3	C46	Sony_W170_1